SLAC-PUB-12988

Radiative and Electroweak Penguin Decays of B Mesons

Jeffrey D. Richman[a] (on behalf of the BaBar and Belle Collaborations)

[a]Department of Physics, University of California, Santa Barbara, CA 93106, USA

Radiative and electroweak penguin decays of B mesons are flavor-changing-neutral-current processes that provide powerful ways to test the Standard Model at the one-loop level, to search for the effects of new physics, and to extract Standard Model parameters such as CKM matrix elements and quark masses. The large data samples obtained by the B-factory experiments BaBar and Belle, together with an intensive theoretical effort, have led to significant progress towards understanding these rare decays. Recent experimental results include the measurements of the $b \to d\gamma$ decays $B \to \rho(\omega)\gamma$, the observation of $B \to K^{(*)}\ell^+\ell^-$ decays (together with studies of the associated kinematic distributions), and improved measurements of the inclusive $B \to X_s\gamma$ rate and photon energy spectrum.

1. INTRODUCTION

Radiative and electroweak penguin decays of B mesons are flavor-changing-neutral current (FCNC) processes that involve $b \to s$ or $b \to d$ transitions. In contrast to the dominant $b \to c$ decays (or the rare $b \to u$ decays), which occur at tree level, FNCN processes are described by loop or box diagrams at leading order in the Standard Model (SM).

The observation of $B \to K^*\gamma$ by the CLEO experiment in 1993 [1] opened up this field and demonstrated that loop processes are indeed present at roughly the rate expected in the SM. The branching fraction $B(B \to K^*\gamma) \approx 4 \times 10^{-5}$, while small, is large enough that thousands of such events are now observed in the B-factory data samples of the BaBar and Belle experiments, which together now contain about 10^9 $\Upsilon(4S) \to B\bar{B}$ events. Since the discovery of $B \to K^*\gamma$, the study of FCNC B decays has expanded into a broad physics program [2] involving electromagnetic, electroweak, and hadronic penguin processes; we discuss the first two of these in this paper.

Figure 1 shows the SM diagrams relevant to the FCNC B decays to final states with photons or leptons. For the $b \to s(d)\gamma$ decay, there is a single diagram, the electromagnetic penguin, while for $b \to s\ell^+\ell^-$, there are three contributing amplitudes, two penguins and a box diagram. A key feature of these processes is that there may be additional, non-SM contributions to the amplitude arising from the presence of new particles in the virtual intermediate state, such as charged Higgs bosons, charginos, neutralinos, gluinos, and squarks.

This talk focuses on three areas of investigation in radiative/electroweak penguin physics:

- Measurement of the rate for $B^+ \to \rho^+\gamma$, $B^0 \to \rho^0\gamma$, and $B^0 \to \omega\gamma$ and the extraction of $|V_{td}/V_{ts}|$,
- Measurement of $B \to K\ell^+\ell^-$ and $B \to K^*\ell^+\ell^-$, and the search for new physics using kinematic distributions,
- Measurement of $B \to X_s\gamma$ inclusive, where the rate provides a key test of the SM, and the photon energy spectrum constrains the b-quark mass m_b and other hadronic parameters.

2. OBSERVATION OF $b \to d\gamma$ AND MEASUREMENT OF $|V_{td}/V_{ts}|$

The ratio of branching fractions for $B \to \rho\gamma$ and $B \to K^*\gamma$ can be expressed in terms of $|V_{td}/V_{ts}|$ using the relation [3]:

Contributed to International Conference on B-Physics at Hadron Machines (Beauty 2006), 09/25/2006--9/29/2006, Oxford, England

Work supported in part by US Department of Energy contract DE-AC02-76SF00515

Table 1
BaBar and Belle results for the branching fractions (B.F.) for the $b \to d\gamma$ decays $B^+ \to \rho^+\gamma$, $B^0 \to \rho^0\gamma$, and $B^0 \to \omega\gamma$. The BaBar results are preliminary. The weighted average given in the last row of the table is based on isospin symmetry and quark-model assumptions discussed in the text.

Mode	B.F./10^{-6} (BaBar)	Signif.	B.F./10^{-6} (Belle)	Signif.
$B^+ \to \rho^+\gamma$	$1.10^{+0.37}_{-0.33} \pm 0.09$	3.8σ	$0.55^{+0.42+0.09}_{-0.36-0.08}$	1.6σ
$B^0 \to \rho^0\gamma$	$0.79^{+0.22}_{-0.20} \pm 0.06$	4.9σ	$1.25^{+0.37+0.07}_{-0.33-0.06}$	5.2σ
$B^0 \to \omega\gamma$	$0.40^{+0.24}_{-0.20} \pm 0.05$	2.2σ	$0.56^{+0.34+0.05}_{-0.27-0.10}$	2.3σ
$B \to (\rho^+, \rho^0, \omega)\gamma$	$1.25^{+0.25}_{-0.24} \pm 0.09$	6.4σ	$1.32^{+0.34+0.10}_{-0.31-0.09}$	5.1σ

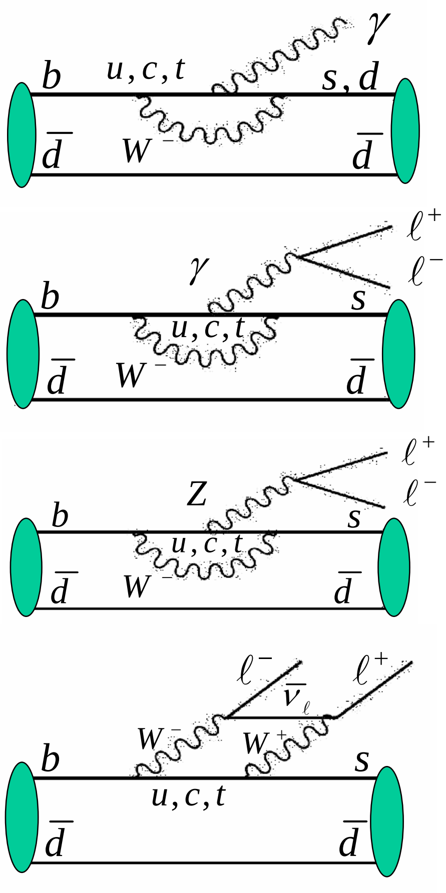

Figure 1. Diagrams for SM contributions to $b \to s\gamma$ and $b \to s\ell^+\ell^-$ decays.

$$\frac{\mathcal{B}(B \to (\rho,\omega)\gamma)}{\mathcal{B}(B \to K^*\gamma)} = \left|\frac{V_{td}}{V_{ts}}\right|^2 \frac{(1 - m^2_{\rho,\omega}/m^2_B)^3}{(1 - m^2_{K^*}/m^2_B)^3} \times \left(\frac{T_1^{\rho,\omega}(0)}{T_1^{K^*}(0)}\right)^2 (1 + \Delta R) \quad (1)$$

where m_i is the mass of particle i, $T_1^\rho(0)$ and $T_1^{K^*}(0)$ are the tensor form factors for $B \to \rho$ and $B \to K^*$ transitions evaluated at four-momentum transfer $q^2 = 0$ (rapid hadronic recoil). The factor $\Delta R = 0.1 \pm 0.1$ [4] parametrizes $SU(3)$ breaking effects and $1/m_b$ power corrections to QCD factorization. The form factor ratio can be predicted more precisely than the individual form factors themselves, but it remains the dominant source of theoretical uncertainty. Using light-cone sum-rule techniques, Ball and Zwicky [3] obtain $T_1^{K^*}(0)/T_1^\rho(0) = 1.17 \pm 0.09$.

The numerator in Eq. 1 refers to both $\rho\gamma$ and $\omega\gamma$ final states. Because the signals are currently very small, current practice has been to use an appropriately weighted average over ρ^+, ρ^0, and ω modes. The weightings are based on the I-spin relation between the decay widths $\Gamma(B^- \to \rho^-\gamma) = 2\Gamma(\bar{B}^0 \to \rho^0\gamma)$, as well as the relation $\Gamma(\bar{B}^0 \to \rho^0\gamma) = \Gamma(\bar{B}^0 \to \omega\gamma)$, which results from the quark-model flavor wave functions of the ρ^0 and ω. Another issue is the presence of an additional amplitude for the $B^- \to \rho^-\gamma$ decay, which receives a small contribution from the annihilation diagram. In principle, this possibility is accounted for by the uncertainty on ΔR. With a large amount of data, however, it would be cleaner to simply use the $B^0 \to \rho^0\gamma$ decay only for the calculation.

The first observation of $b \to d\gamma$ decays was made by Belle using a sample of 386M $B\bar{B}$ events [5]. The number of signal events in the three modes is $\rho^-\gamma$ (8.5), $\rho^0\gamma$ (20.7), and $\omega\gamma$ (5.7), for a combined significance of 5.1σ. Based on a sample of 347M $B\bar{B}$ events, BaBar has obtained [6] signals with a combined significance of 6.4σ. These measurements are complicated by the small branching fractions, the large background from continuum ($e^+e^- \to q\bar{q}$) processes, and peaking background from misidentified $B \to K^*\gamma$ events.

Table 1 lists BaBar and Belle results for the individual $b \to s\gamma$ modes and for the combined average (expressed as a $B^+ \to \rho^+\gamma$ result), using the theoretical relations discussed above. The $B \to \rho^+\gamma$ branching fraction is about 3% of that for $B \to K^*\gamma$, giving a rough indication of the effect of $|V_{td}/V_{ts}|^2$. Interestingly, the Belle branching fraction for $B^0 \to \rho^0\gamma$ is about twice that for $B^- \to \rho^-\gamma$, the inverse of the expectation from isospin symmetry. The Belle paper reports a probability of 4.9% for the observed "isospin violation" to be equal or larger than what is measured. The BaBar data, however, do not exhibit this behavior and are consistent with isospin symmetry. This situation merits examination with more data. For the present, it has been the assumption to assume isospin symmetry and to regard the Belle pattern of branching fractions as simply a statistical fluctuation.

Using Eq. 1, one can then extract

$$\left|\frac{V_{td}}{V_{ts}}\right| = 0.199^{+0.026+0.018}_{-0.025-0.015} \text{ (Belle)}$$
$$= 0.200^{+0.021}_{-0.020} \pm 0.015 \text{ (BaBar)}. \qquad (2)$$

Within their uncertainties, these values are consistent with the recent CDF measurement [7] using B_s mixing:

$$|V_{td}/V_{ts}| = 0.208^{+0.001}_{-0.002}(\text{exp})^{+0.008}_{-0.006}(\text{theo}) \text{ (CDF)}. \quad (3)$$

It is notable that these two methods for extracting $|V_{td}/V_{ts}|$, which are made using different physical processes with different theoretical uncertainties, yield consistent results.

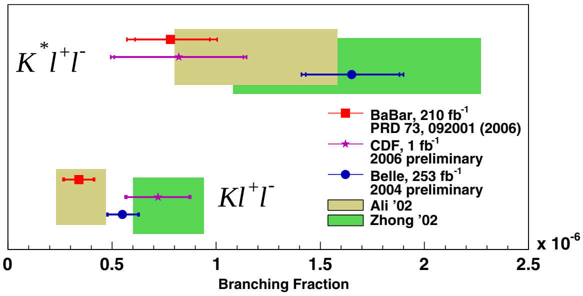

Figure 2. Summary of measured branching fractions for $B \to K\ell^+\ell^-$ and $B \to K^*\ell^+\ell^-$.

3. $B \to K\ell^+\ell^-$ AND $B \to K^*\ell^+\ell^-$ IN THE STANDARD MODEL AND BEYOND

In contrast to $B \to K^*\gamma$, which is purely an electromagnetic penguin process, three distinct electroweak amplitudes contribute to the decays $B \to K^{(*)}\ell^+\ell^-$ in the SM. These are shown in Fig. 1 and are the photon penguin, the Z penguin, and the W^+W^- box diagram. While the photon penguin is the most familar, its contribution is important only in the low q^2 region of phase space. The amplitude for $B \to K^*\ell^+\ell^-$ is [8]

$$\mathcal{M}(B \to K^*\ell^+\ell^-) = \frac{G_F\alpha_{\rm EM}}{\sqrt{2}\pi}V_{ts}^*V_{tb}$$
$$\times\{[C_9^{\rm eff}\langle K^*|\bar{s}\gamma_\mu P_L b|B\rangle$$
$$-2\frac{m_b}{q^2}C_7^{\rm eff}\langle K^*|\bar{s}i\sigma_{\mu\nu}q^\nu P_R b|B\rangle]\left(\bar{\ell}\gamma^\mu\ell\right)$$
$$+C_{10}\langle K^*|\bar{s}\gamma_\mu P_L b|B\rangle\left(\bar{\ell}\gamma^\mu\gamma_5\ell\right)\}, \qquad (4)$$

where P_L and P_R are the left- and right-handed chirality projection operators. In this expression, the short-distance physics is parametrized by the Wilson coefficients C_i, which have been calculated at next-to-next-to leading order (NNLO) in the SM: $C_7^{\rm eff} = -0.3$, $C_9 = +4.3$, and $C_{10} = -4.7$. The term containing $C_7^{\rm eff}$ represents the photon penguin amplitude, which is proportional to $1/q^2$. The terms containing C_9 and C_{10} are each a mix of the amplitudes associated with the Z penguin and the W^+W^- box diagram. New physics can enter at the same order as SM processes, potentially modifying the C_i's.

The hadronic matrix elements in Eq. 4 involve long-distance QCD interactions. These interactions are described in terms of form factors, which are functions of $q^2 = (p_{\ell+} + p_{\ell-})^2$, where $p_{\ell+-}$ are the leptonic four-vectors. For $B \to K^*\ell^+\ell^-$, there are four semileptonic form factors (A_1, A_2, V, A_0), which are similar to those that enter the amplitudes for $B \to K^*\ell^-\bar{\nu}$ and $B \to \rho\ell^-\bar{\nu}$, and three penguin form factors (T_1, T_2, and T_3). Most of the theoretical uncertainty in the rates is due to uncertainty in these form factors.

Figure 2 summarizes the status of the branching fraction measurements from BaBar, Belle, and CDF. BaBar [9] and Belle [10] have observed these processes for some time and have recently published results on kinematic distributions. CDF has just observed these processes and has presented preliminary results [11]. Averaging the BaBar and Belle measurements, the Heavy Flavor Averaging group [2] obtains the branching fractions $B(B \to K\ell^+\ell^-) = (0.442 \pm 0.052) \times 10^{-6}$ and $B(B \to K^*\ell^+\ell^-) = (1.17 \pm 0.16) \times 10^{-6}$. The decay $B \to K\ell^+\ell^-$ has the smallest branching fraction of any observed B decay. The BaBar and Belle measurements for $B \to K^*\ell^+\ell^-$ are in somewhat marginal agreement, but this should be resolved with more data.

In $B \to K^*\ell^+\ell^-$, the lepton forward-backward asymmetry in the dilepton rest frame, A_{FB}, has particularly interesting properties, because it is very sensitive to the interference between the different amplitudes in Eq. 4. The amplitudes are a function of q^2, and the dependence of A_{FB} on q^2 reveals not only the magnitudes of the C_i, but also provides information on their relative signs.

For a B meson containing a b quark (B^- or $\bar{B}^0$), A_{FB} can be defined as follows using the negative lepton ℓ^-. Take the $+z$ axis in the $\ell^+\ell^-$ rest frame to be aligned with the direction of the dilepton system in the B rest frame. The asymmetry is then $A_{FB} = (N_F - N_B)/(N_F + N_B)$, where N_F and N_B are the number of negative leptons in the forward ($+z$) hemisphere and backward $-z$ hemispheres, respectively. At very low q^2, the SM predicts $A_{FB} < 0$ as a consquence of interference between the C_7 and C_{10} terms. The

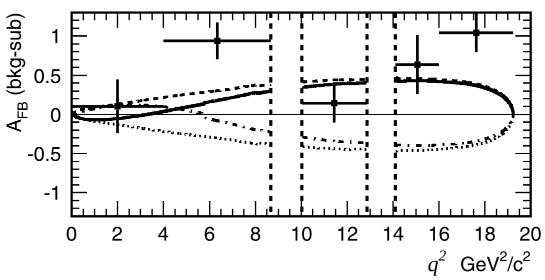

Figure 3. Measurement of the lepton-forward backward asymmetry, A_{FB}, for the decay $B \to K^*\ell^+\ell^-$, from Belle. The measurements are shown as points with error bars in five bins of q^2. The SM prediction is the solid curve, while several alternative values for the Wilson coefficients lead to the other curves.

asymmetry is predicted to be zero at $q^2 = q_0^2 = 4.07^{+0.16}_{-0.13}$ GeV^2 [12] and then to be positive for $q^2 > q_0^2$ due to interference between C_9 and C_{10}.

Both BaBar [9] and Belle [10] have performed detailed studies of A_{FB} in bins of q^2. BaBar has also measured the polarization of the K^*. Because the branching fractions for these modes are small, the statistical precision is limited. In addition, the q^2 regions corresponding to $m^2_{\ell^+\ell^-} = m^2_{J/\psi}$ and $m^2_{\ell^+\ell^-} = m^2_{\psi(2S)}$ must be vetoed due to huge backgrounds from $B \to J/\psi K^{(*)}$, $J/\psi \to \ell^+\ell^-$. Nevertheless, these studies provide a first look at the kinematic behavior of $B \to K^*\ell^+\ell^-$ and $B \to K\ell^+\ell^-$. Figure 3 shows the Belle results for A_{FB} in bins of q^2. The data show positive values of A_{FB} over most of the q^2 range, in agreement with the SM. BaBar observes similar behavior, measuring $A_{FB}(q^2 > 10.42\,\text{GeV}^2) = +0.72^{+0.28}_{-0.26} \pm 0.08$. Belle obtains $A_{FB} = +0.50 \pm 0.15 \pm 0.02$ (full q^2 range) and has fit for individual Wilson coefficients. Models that predict $A_{FB} < 0$ in the upper q^2 range are disfavored by both experiments. In the low q^2 range, the BaBar data show a value of A_{FB} greater than that expected in the SM, but the statistical uncertainty is large. Belle has performed a joint fit to the distributions of q^2 and $\cos\theta_\ell$ and finds values of the Wilson coefficients that are consistent with the SM. For the decay $B \to K\ell^+\ell^-$, both experiments measure A_{FB} consistent with zero, in agreement with the SM.

The signal yields used in these measurements are small, around 50 to 100 events, and there is clearly much more to be learned with more data. Studies of these distributions will be performed for many years to come, at the B-factories, the Tevatron, and at LHCb.

4. INCLUSIVE $B \to X_s\gamma$

The inclusive decay $B \to X_s\gamma$ is a canonical process for studying the $b \to s$ transition [13]. The theoretical challenge of evaluating the QCD corrections involves calculating hundreds or even thousands of Feynman diagrams [16]. Theoretical uncertainties in NLO calculations are around the 10% level and NNLO calculations currently underway are expected to reach the 5% level of precision. Although the photon energy spectrum is insensitive to new physics, it is still of great interest because it can be used to extract m_b, as well as information on the Fermi motion of the b-quark. Examples of theoretical predictions are given in Table 2.

Experimentally, there are two approaches to $B \to X_s\gamma$. The fully inclusive approach, which relies on the high-energy photon and event-shape characteristics, is conceptually the most appropriate, because the final state X_s is not in any way restricted. This method suffers from large backgrounds. An alternative, which has a stronger experimental signature, is to sum over as many exclusive modes as possible. In a recent BaBar measurement [17], 38 exclusive modes were summed. Although the signal is cleaner, the limited set of reconstructable final states inevitably introduces a significant degree of model dependence.

BaBar [18], Belle [19], and CLEO [20] have all performed measurements of $B(B \to X_s\gamma)$ using some version of the fully inclusive method. Recently, BaBar has performed an analysis in which a high-momentum lepton, which comes from the other B in signal events, is used to suppress continuum background. Figure 4 shows

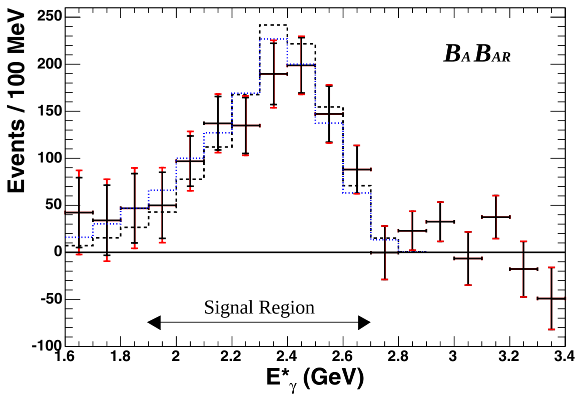

Figure 4. Photon energy spectrum for the process $B \to X_s\gamma$ from the BaBar fully inclusive measurement with a lepton tag. The spectrum (points with error bars) is given in the $\Upsilon(4S)$ rest frame and is not efficiency corrected. The histograms show theoretical predictions based on the best fit using shape functions in the kinetic scheme (dashed histogram) and the shape function scheme (dotted histogram). These predictions include the effects of detector acceptance and analysis efficiency.

the photon energy E_γ spectrum from this measurement. The branching fraction is measured for $E_\gamma > 1.9$ GeV and is extrapolated down to $E_\gamma = 1.6$ GeV, yielding $B(B \to X_s\gamma) = (3.94 \pm 0.31 \pm 0.36 \pm 0.21) \times 10^{-4}$ if the kinetic-scheme shape function is used. The substantial systematic uncertainties are typical of $B \to X_s\gamma$ measurements. The world-average experimental value computed by HFAG [2] for $E_\gamma > 1.6$ GeV is $B(B \to X_s\gamma) = (3.55 \pm 0.24^{+0.09}_{-0.10} \pm 0.03) \times 10^{-4}$, where the first error is the combined statistical and systematic experimental uncertainty, the second error is associated with shape-function assumptions, and the third is due the correction for the $b \to d\gamma$ contribution. At the present level of precision, this value is in good agreement with the theoretical predictions given in Table 2.

While the branching fraction provides a stringent test of the SM at the one-loop level, the pho-

Table 2
Predictions for $B \to X_s\gamma$. The uncertainties in the Hurth *et al.* result are m_c/m_b, CKM, parameter dependence, and scale dependence.

Ref.	$B(B \to X_s\gamma)/10^{-6}$
Hurth *et al.* [14]	$3.61^{+0.24}_{-0.40} \pm 0.02 \pm 0.24 \pm 0.14$
Neubert [15]	$3.47^{+0.33}_{-0.41}\vert_{\rm pert}{}^{+0.32}_{-0.29}\vert_{\rm param}$
Misiak *et al.* [16]	3.15 ± 0.23

ton energy spectrum provides important information on the b-quark mass. Using the moments of lepton-energy spectrum from $B \to X_c\ell^-\bar{\nu}$ and of the photon energy spectrum from $B \to X_s\gamma$, several authors have extracted m_b, m_c, $|V_{cb}|$, and other parameters describing the hadronic physics of the B meson to remarkable precision. In addition, the value of m_b is also important for determinations of $|V_{ub}|$ using inclusive $B \to X_u\ell^-\bar{\nu}$ measurements. An example of such an analysis is the paper by Buchmüller and Flächer [21], who use theoretical input from Gambino and Uraltsev [22] and experimental input from BaBar, Belle, CDF, CLEO, and DELPHI to extract $m_b = 4.590 \pm 0.025\,(\mathrm{exp}) \pm 0.030\,(\mathrm{HQE})$ GeV in the kinetic scheme. HQE refers to uncertainties associated with the heavy quark expansion.

5. CONCLUSIONS AND PROSPECTS

Studies of radiative and electroweak penguin decays have moved far beyond the observation of $B \to K^*\gamma$. This field will benefit greatly from the large increases in the data samples forseen for the future at the B factories, the Tevatron, and at LHCb, as well as from the critical contributions of our theoretical colleagues.

Acknowledgments

I would like to thank the organizers for a superbly organized and run conference.

REFERENCES

1. CLEO Collaboration, R. Ammar *et al.*, Phys. Rev. Lett. **71** (1993) 674.
2. Heavy Flavor Averaging Group, E. Barberio *et al.*, hep-ex/0603003, updated (ICHEP06): http://www.slac.stanford.edu/xorg/hfag/
3. P. Ball and R. Zwicky, Journal of High Energy Physics 0604 (2006) 046, [arXiv:hep-ph/0603232].
4. A. Ali, E. Lunghi, and A. Parkhomenko, Phys. Lett. **B 595** (2004) 323 [arXiv:hep-ph/0405075]. A more extensive list of references is given in Ref. [3].
5. Belle Collaboration, D. Mohapatra *et al.*, Phys. Rev. Lett. **96** (2006) 221601.
6. BaBar Collaboration, B. Aubert *et al.*, BABAR-PUB-06/070, hep-ex/0612017, accepted by PRL.
7. CDF Collaboration, A. Abulencia *et al.*, Phys. Rev. Lett. **97** (2006) 062003.
8. F. Kruger and J. Matias, Phys. Rev. **D 71** (2005) 094009.
9. BaBar Collaboration, B. Aubert *et al.*, Phys. Rev. **D 73** (2006) 092001.
10. Belle Collaboration, A. Ishikawa *et al.*, Phys. Rev. Lett. **96** (2006) 251801.
11. Cheng-Ju S. Lin, these proceedings.
12. A. Ali, G. Kramer, and G. Zhu, Eur. Phys. J **C 47** (2006) 625.
13. T. Hurth, Rev. Mod. Phys. **75** (2003) 1159.
14. T. Hurth, E. Lunghi, W. Porod, Nucl. Phys. **B 704** (2005) 56.
15. M. Neubert, Eur. Phys. J. **C 40** (2005) 165.
16. M. Misiak *et al.*, arXiv:hep-ph/0609232.
17. BaBar Collaboration, B. Aubert *et al.*, Phys. Rev. **D 72** (2005) 052004.
18. BaBar Collaboration, B. Aubert *et al.*, Phys. Rev. Lett. **97** (2006) 171803.
19. Belle Collaboration, P. Koppenburg *et al.*, Phys. Rev. Lett. **93** (2004) 061803.
20. CLEO Collaboration, S. Chen *et al.*, Phys. Rev. Lett. **87** (2001) 251807.
21. O. Buchmüller and H. Flächer, Phys. Rev. D **73** (2006) 073008.
22. P. Gambino and N. Uraltsev, Eur. Phys. J **C 34** (2004) 181.